DERIVATION OF FURROW GEOMETRY USING ENTROPY THEORY

V. P. Singh

ABSTRACT. *Furrow irrigation is one of the commonly used surface irrigation methods. Design of furrow irrigation requires determination of furrow geometry. The usual practice in irrigation design is to specify furrow geometry empirically, even though hydraulic principles can be applied to derive furrow geometry. This study derives irrigation furrow geometric parameters using entropy theory and evaluates these parameters with observations from nine field sites each with five irrigation events in a field laboratory. Comparison of computed geometric parameters and observed values shows a good agreement and points to the potential that entropy theory might have in irrigation modeling. Because entropy is a measure of uncertainty, the use of entropy theory may allow description of the uncertainty associated with furrow geometry and in turn with furrow irrigation efficiency.*

Keywords. *Entropy, Furrow, Geometry, Lagrange multiplier, Principle of maximum entropy, Shannon entropy, Surface irrigation.*

Furrow geometry is fundamental to the development of furrow irrigation systems. Calculation of hydraulic characteristics, such as depth, velocity, and cross-sectional area of flow; discharge; surface storage; infiltration; and friction requires furrow geometry. Different types of furrow shapes have been employed in furrow irrigation modeling. Under the assumption that the furrow shape does not change in time, figure 1a represents a typical cross-sectional shape. This kind of shape is encountered at the head, at the midpoint, and at the outflow end of a furrow.

Several furrow cross-sectional shapes have been used, such as rectangular, triangular, trapezoidal, and parabolic. These shapes have often been used to approximate natural channel sections (Chow, 1959). King (1939) found that a parabolic section approximated the form assumed by many natural streams and old canals. The USDA Soil Conservation Service (now the National Resources Conservation Service; SCS, 1983) employed a trapezoidal shape to derive relationships between geometric parameters and irrigation design procedure. The commonly used shape, however, is a power function (Fangmeier and Ramsey, 1978; Elliott et al., 1983; Trout, 1991). The usual procedure is to assume a two-parameter power function for shape and then estimate its parameters using a least square method or express the power function with measured values at two points and then solve the two equations for parameters. This is one of the cross-sectional shapes of stable alluvial channels (Henderson, 1966).

If the soil in which furrows are constructed is not a stable medium, which is the case most of the time, soil particles, detached by shear and sloughing, are transported and washed away by flow of water. Usually, fine particles are transported by water, and coarser particles accumulate in the channel bed. The furrow shape eventually changes to a hydraulically stable shape. The stability depends on the distribution and magnitudes of forces, the size and stability of the soil aggregates, and the cohesion (structure and texture) of the soil (Foster and Lane, 1983; Lane and Nearing, 1989; Trout, 1991). Erosion from side walls causes furrows to widen and decreases the bed slope; this leads to increased flow depth, thus maintaining approximately the same shape. If the slope increases because of bed erosion, the flow velocity will increase but the flow depth will decrease, resulting in a smaller cross-section and a narrower wetted perimeter. Thus, the evolution of furrow geometry involves a number of factors, including soil properties and hydraulics of flow, and their interactions. In the discussion in this article, however, these factors will not be explicitly considered.

Furrow geometry parameters include side slope, shape, cross-section, flow depth, wetted perimeter, width, and hydraulic radius. These parameters are required for furrow ir-

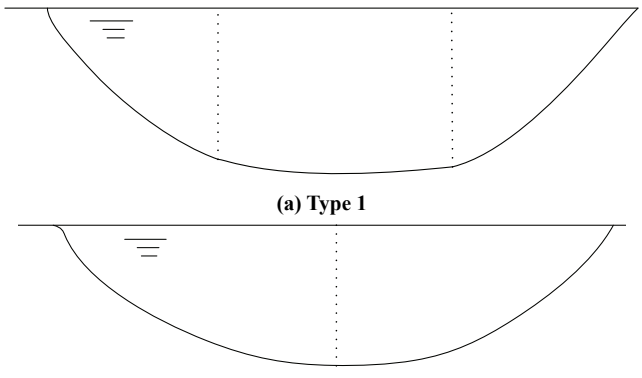

(a) Type 1

(b) Type 2

Figure 1. Furrow geometry.

Submitted for review in December 2012 as manuscript number SW 9536; approved for publication by the Soil & Water Division of ASABE in May 2012.

The author is **Vijay P. Singh,** Caroline & William N. Lehrer Distinguished Chair in Water Engineering, Professor, Department of Biological and Agricultural Engineering, and Professor, Department of Civil and Environmental Engineering, Texas A&M University, 321 Scoates Hall, 2117 TAMU, College Station, TX 77843-2117; e-mail: vsingh@tamu.edu.

  ISSN 2151-0032

rigation modeling and evaluation. For example, infiltration area is usually related to wetted perimeter. Hydraulic radius is used to compute tractive force needed for erosion models. Flow depth is needed to compute water surface elevation and hence the energy or friction slope in hydrodynamic irrigation models. These parameters are computed in two ways. First, an assumed shape is fitted to empirical field or laboratory observations, and then parameters are derived for the empirically fitted shape. Second, for an assumed furrow shape, a hydraulic flow equation, such as the Manning or Chezy equation, is used to relate geometric parameters to hydraulic parameters. For simplicity, the assumed or empirically fitted shape is assumed to remain fixed for the furrow irrigation system under consideration, even though it is known that a furrow shape varies in time and space and these variations have a great deal of randomness. Because these methods are deterministic, nothing can be said about the uncertainty associated with furrow parameters. The objective of this article, therefore, is to employ a probabilistic approach based on entropy theory to derive furrow geometry characteristics, test these characteristics using laboratory furrow measurements, and discuss their probabilistic characteristics.

Derivation of Furrow Geometry Using Entropy Theory

Before applying entropy theory to the derivation of furrow geometry parameters, it is necessary to state what the random variable is and what assumptions need to be made regarding the furrow (or channel) shape.

Assumptions

In order to derive furrow geometry parameters, it is assumed that the shape of the channel is curved, as shown in figure 1b. Thus, the distribution of transverse slopes needs to be determined, and this will then lead to the bank profile of the furrow cross-section. It is assumed that the dimensions and shape depend on the discharge and boundary sediment size or angle of repose of particles. Furthermore, the two bank profile curves on the sides of the centerline meet at the centerline, and the shape curve must satisfy the continuity at the meeting point. The shape on either side of the centerline is assumed to be the same for purposes of simplicity. The elevation from the horizontal datum to the bank is denoted as y, varying from 0 to D at the water surface ($0 \le y \le D$).

Definition of Variables

Let x be the lateral distance from the centerline, varying from 0 to W, where W is the half channel width from the centerline. The total width of the channel would then be $2W$, or B. The flow depth is denoted as h, varying from 0 to h_c, which equals D, where D is the bankful flow depth at the centerline. The transverse slope is denoted by $s = \tan\theta = dy/dx$ varying from 0 to s_0, where s is the submerged coefficient of friction, y is the elevation of the bank at x, and s_0 is the maximum slope equal to the angle of repose μ, the angle of internal friction for sediment, or the static coefficient of Coulomb friction, as shown in figure 2. It is assumed that the transverse slope increases monotonically from the centerline to the water surface. Furthermore, the transverse slope is found to vary from one cross-section to another. In other words, it has spatial variability. Therefore, it is not unduly restrictive to assume that the transverse slope is a random variable denoted as S.

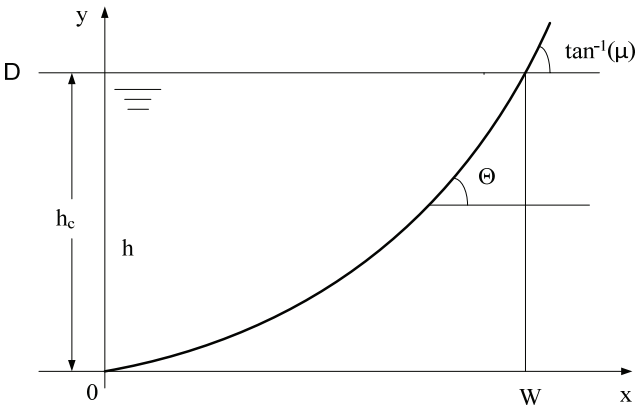

Figure 2. Half channel width and notations.

Steps for Derivation

The entropy-based derivation of furrow geometric parameters entails (1) defining the Shannon entropy, (2) specification of constraints, (3) entropy maximizing using the method of Lagrange multipliers and determination of probability density function of transverse slope, (4) determination of Lagrange multipliers, (5) hypothesis for distribution of transverse slope, and (6) determination of cross-section shape and geometry parameters. Each of these steps is now discussed in what follows.

Shannon Entropy

The Shannon entropy (Shannon, 1948) of the transverse slope can be expressed as:

$$H(S) = -\int_0^{s_0} f(s)\ln f(s)\,ds \tag{1}$$

where s is the value of random variable S, $f(s)$ is the probability density function (PDF) of S, and H is the entropy of S or $f(s)$. Equation 1 is a measure of uncertainty of $f(s)$ or variable S. The objective is to derive $f(s)$ by maximizing H, subject to specified constraints, in accordance with the principle of maximum entropy (POME) (Jaynes, 1957). The reason for maximizing the entropy is that the derived probability distribution of slope should be based on only what is specified *a priori* and nothing else. This will allow the probability distribution to be least biased toward what is not specified.

Specification of Constraint

For purposes of simplicity, the constraint that $f(s)$ must satisfy is formulated as:

$$\int_0^{s_0} f(s)\,ds = 1 \tag{2}$$

which is the total probability theorem. In a sense, this is really not a constraint because all probability distributions must satisfy it. Other constraints, such as mean, variance, skewness, etc., can be specified, but their values may not be known beforehand and it may be preferable to first keep the analysis simple without undue loss of accuracy. Thus, nothing is being assumed about the furrow side slope.

Entropy Maximizing and Probability Density Function

The least-biased probability distribution function $f(s)$ is obtained by maximizing entropy given by equation 1, subject to equation 2. This is done by using the method of Lagrange multipliers, where the Lagrangean function L can be expressed as:

$$L = -\int_0^{s_0} f(s)\ln f(s)ds - (\lambda_0 - 1)(\int_0^{s_0} f(s)ds - 1) \tag{3}$$

where λ_0 is the Lagrange multiplier. Differentiating equation 3 with respect to f, while recalling the Euler-Lagrange calculus of variation, noting that f is variable and s is a parameter, and equating the derivative to zero, one obtains:

$$\frac{\partial L}{\partial f} = 0 \Rightarrow -\ln f(s) - \lambda_0 = 0 \tag{4}$$

Equation 4 yields:

$$f(s) = \exp(-\lambda_0) \tag{5}$$

Equation 5 is a uniform density function (PDF) of transverse slope S. The cumulative distribution function (CDF) of S is obtained by integrating equation 5:

$$F(s) = \exp(-\lambda_0)s \tag{6}$$

Equation 6 is linear, implying that all values of slope are equally likely.

The maximum entropy of S is obtained by inserting equation 5 in equation 1:

$$H(s) = \lambda_0 \exp(-\lambda_0)s_0 \tag{7}$$

which is expressed in terms of the Lagrange multiplier λ_0 and constant s_0. Equation 7 reflects the maximum uncertainty about the side slope.

Determination of the Lagrange Multiplier

Substitution of equation 5 in equation 2 yields:

$$\exp(-\lambda_0) = \frac{1}{s_0} \tag{8}$$

Therefore:

$$\lambda_0 = \ln s_0 \tag{9}$$

Substitution of equation 8 in equation 5 leads to the PDF of S as:

$$f(s) = \frac{1}{s_0} \tag{10}$$

Equation 10 states that the PDF of S is uniform. Likewise, substitution of equation 8 in equation 6 yields the CDF of S:

$$F(s) = \frac{s}{s_0} \tag{11}$$

Equation 11 states that the CDF of S is linear bounded by the upper limit, s_0. Similarly, substitution of equations 8 and 9 in equation 7 yields:

$$H(s) = \ln s_0 \tag{12}$$

It is interesting to note that the uncertainty about the slope depends only on the knowledge of the upper limit of S, which is s_0. Therefore, it is important to specify the value of s_0 as accurately as possible. It may be noted that the uncertainty in slope will change if more characteristics of slope are to be preserved, that is, more constraints on slope are specified.

Hypothesis for Distribution of Transverse Slope

At any lateral distance from the centerline less than x, the transverse slope at that distance is less than s. It can then be reasoned that all values of x between 0 and W along the x-axis are equally likely to be sampled or have the same probability. Therefore, the probability of the transverse slope being equal to or less s is x/W. The cumulative distribution function (CDF) of S can then be expressed in terms of the lateral or transverse distance as:

$$F(s) = \frac{x}{W} \tag{13}$$

Equation 13 is just a hypothesis, and its validity in the field needs to be tested. Further, one can express a more general hypothesis of which equation 13 can be a special case (Singh, 2011).

Differentiating equation 13 yields the PDF of S as:

$$f(s)ds = \frac{1}{W}dx$$

or

$$f(s) = \frac{1}{W}\frac{dx}{ds} = \left(W\frac{ds}{dx}\right)^{-1} \tag{14}$$

The PDF given by equation 5 must satisfy the constraint defined by equation 2. Inserting equation 10 in equation 14, one gets:

$$\frac{1}{s_0} = \frac{1}{W}\frac{dx}{ds} \tag{15}$$

Integration of equation 15 yields:

$$s = \frac{s_0}{W}x \tag{16}$$

Equation 16 expresses the distribution of transverse slope as a function of transverse distance, and satisfies the condition that $s = 0$ at $x = 0$ and $s = s_0$ at $x = W$. Equation 16 assumes that the side slope of the furrow varies only with the transverse distance, given the values of the half width and the maximum slope. Further, it assumes that the furrow

cross-section is the same. Of course, this assumption can be relaxed, but the algebra becomes complicated. The values of s_0 and W can be determined beforehand for a given soil and crop irrigation requirements. Each soil has an angle of friction, and the maximum side slope will be bounded by this angle. For a given crop, the furrow size can be specified. In many developing countries, furrows are constructed manually. The furrow size also depends on the equipment at hand. Equation 16 is a simple expression and can be easily used for furrow design and construction in the field. Of course, this equation may not be valid for all soils under all conditions. It may be further noted that derivation of equation 16 entails a simple hypothesis expressed by equation 13 and specification of slope between zero and an upper limit in correspondence with a specified soil, but no constraints on slope itself. Under the condition treated here for purposes of simplicity, it is plausible to derive equation 16 without the use of entropy theory. However, if a more complicated case is analyzed, that is, constraints on slope, such as mean, variance, skewness, etc., are introduced, then entropy theory may be the most viable approach to derive slope and consequent furrow geometry characteristics.

Cross-Section Shape and Geometric Parameters

The furrow geometric parameters of interest are shape, centerline flow depth, flow depth, aspect ratio, cross-section area, wetted perimeter, and hydraulic radius.

Shape function: Recall the definition of slope, $s = dy/dx$; equating it to equation 16, one gets:

$$\frac{dy}{dx} = \frac{s_0}{W}x \tag{17}$$

Integrating equation 17 with the condition that $s = 0$ at $x = 0$, the bank profile becomes:

$$y = \frac{s_0}{2W}x^2 \tag{18}$$

Equation 18 gives the elevation of the right bank or water margin as a function of transverse distance x from the centerline up to $x = W$. For a given furrow cross-section, there is a finite width at the bottom, and therefore $x = x_0$ at $s = 0$. Hence, for computing the flow depth, equation 18 should be modified as:

$$y = \frac{s_0}{2W}(x - x_0)^2 \tag{18a}$$

Equation 18 is the derived shape function $y = y(x)$.

Centerline flow depth: At $x = W$, $y = D$, which is also the flow depth at the centerline h_c and is given by equation 18 as:

$$D = h_c = \frac{s_0 W}{2} \tag{19}$$

Flow depth: Subtracting equation 18 from equation 19, one gets the lateral distribution of local water flow depth as:

$$h = D - y = \frac{s_0}{2}\left(W - \frac{x^2}{W}\right) \tag{20}$$

Equation 19 specifies the depth at the centerline, and equation 20 specifies the boundary elevation at the bed. Taking the difference of these two equations results in the lateral distribution of flow depth $h(x)$ as a function of lateral distance as:

$$h(x) = \frac{s_0 W}{2}\left[1 - \left(\frac{x}{W}\right)^2\right] \tag{21a}$$

For computing depth, equation 21a should be modified as:

$$h(x) = \frac{s_0 W}{2}\left[1 - \left(\frac{x - x_0}{W}\right)^2\right] \tag{21b}$$

Aspect ratio: The aspect ratio $B/D = 2W/D$ then becomes:

$$\frac{B}{D} = \frac{4}{s_0} \tag{22}$$

Cross-section area: Noting that $hdx = dA$, the cross-sectional area A can be obtained by integrating equation 21a as:

$$A = \frac{2}{3}s_0 W^2 \tag{23}$$

Wetted perimeter: The wetted perimeter P_w is computed as follows. Consider an arc element of wetted perimeter $dP_w = (dx^2 + dy^2)^{1/2}$. From equation 18, $dy = x^2 s_0/(2W)$. Therefore, $dy = xs_0 dx/W$, and:

$$dP_w = \left[dx^2 + \left(\frac{xs_0}{W}dx\right)^2\right]^{1/2} = \left[1 + \frac{x^2 {s_0}^2}{W^2}\right]dx$$
$$= \left(\frac{s_0}{W}\right)\left[\left(\frac{W^2}{{s_0}^2}\right) + x^2\right]dx \tag{24}$$

Integrating equation 24 leads to:

$$P_w = \frac{L}{s_0}\left\{s_0\sqrt{1 + {s_0}^2} + \ln\left[s_0 + \sqrt{1 + {s_0}^2}\right]\right\}$$
$$= \frac{2h_c}{{s_0}^2}\left\{s_0\sqrt{1 + {s_0}^2} + \ln\left[s_0 + \sqrt{1 + {s_0}^2}\right]\right\} \tag{25}$$

Hydraulic radius: The hydraulic radius R can be expressed as:

$$R = \frac{2s_0 L^2}{3P_w} = \frac{8{h_c}^2}{3s_0 P_w} \tag{26}$$

TESTING

LABORATORY DATA

Furrow data were obtained from Mailapalli (2006), who conducted furrow experiments on a 4 m × 60 m plot in the Field Water Management Laboratory of the Department of Agricultural and Food Engineering at the Indian Institute of

Technology in Kharagpur, India. The experimental plot contained three 40 m long free-draining furrows of parabolic shape, having a width of 0.30 m and a depth of 0.15 m. The furrows had a center-to-center distance of 0.8 m and a slope of 0.5%. The center furrow was considered as the study furrow and the two side furrows served as the buffer to the center furrow. The furrow experiments were conducted on 6, 17, 21, and 29 February 2004 using constant inflow rates of 0.2, 0.3, 0.4, and 0.5 L s^{-1}, respectively, on the bare furrow field. In 2005, the field was cropped with sunflower (*Helianthus annuus* L.) in four rows having plant-to-plant and row-to-row spacing of 45 and 50 cm, respectively. The sowing was done on 27 February 2005. Experiments were conducted on 3 March, 30 March, 9 April, 16 May, and 23 May 2005 using constant inflow rates of 0.7, 0.6, 0.5, 0.4, and 0.3 L s^{-1}, respectively. It may be noted that the local weather is usually dry during the months of February through May. The constant inflow rates were set before each irrigation event with digital flowmeters. The outflow from the study furrow was collected in two rectangular tanks of 1 m × 1 m × 1 m size, made of acrylic sheets, that were buried at the tail end. The runoff volume was estimated using the water levels measured with a metallic scale at regular intervals from the tanks during the experiment.

Along the length of the center furrow, four locations were identified as S_1, S_2, S_3, and S_4 at 0.5, 13, 26, and 39.5 m, respectively, from the head end of the field. At these locations, furrow cross-section, depth, and velocity of water in the furrow were measured. The percentage vegetation cover developed along the study furrow was also determined for these locations before each irrigation event under cropped field condition.

The furrow cross-section was measured before each irrigation using a profilometer. The profilometer consisted of 15 slots spaced at 0.02 m intervals. The furrow cross-section was measured in terms of the length of the M.S rods that were inserted through the slots to the furrow surface. Thus, the furrow cross-section data for each location consisted of 15 data points. Each data point included the horizontal distance and corresponding furrow depth. The flow depth during an irrigation event was measured at the four locations using a point gauge and the cross-section data. The depth of the water surface from the ridge was determined in terms of the length of the pointer at 15 min intervals. The flow depth in the furrow at each location was determined by subtracting the pointer length from the furrow depth measured prior to the irrigation event. The flow velocity at the four locations was determined using color dye. At 15 min intervals, a drop of dye was placed at a location, and the time taken by the tip of the colored water to travel 1 m along the furrow was noted. The mean velocity of flow was determined by multiplying the measured velocity by a factor of 0.7 (Abrahams et al., 1986).

The vegetation (weed) cover developed in the study furrow was determined as the average percentage cover along the furrow using a rectangular frame (15 cm × 30 cm) that was divided into 18 smaller squares of 5 cm × 5 cm. The rectangular frame was placed at these locations, and the percentage of vegetation cover was estimated for each small square by visual observation. The average of these 18 readings gave the average percentage vegetation cover developed at a location. The average of these four locations was then considered as the percentage of vegetation cover. In all, five irrigation events at nine channel sites were considered. The slope of the given data set varied between 1.3% and 2.4%, as given in table 1.

Table 1. Furrow slope data.

Site	Date (2004) and Flow Rate (L s^{-1}) 6 Feb. (0.2)	17 Feb. (0.3)	21 Feb. (0.4)	29 Feb. (0.5)	8 Mar. (0.2)	Mean	x_0 (cm)
1	1.75	1.75	1.75	1.75	1.725	1.75	4
2	1.575	1.575	1.575	1.5	1.375	1.52	2
3	1.875	1.875	1.875	1.9	1.925	1.89	4
4	1.575	1.575	1.575	1.55	1.6	1.58	4
5	1.575	1.625	1.625	1.75	1.625	1.64	6
6	1.375	1.375	1.375	1.375	1.4	1.38	0
7	1.75	1.75	1.75	1.775	1.75	1.76	8
8	1.6	1.6	1.6	1.475	1.5	1.56	0
9	2.275	2.275	2.275	2.35	2.3	2.30	4

Comparison with Laboratory Data

Fundamental to the computation of the furrow geometric parameters was the calculation of the Lagrange multiplier λ_0, which was computed using equation 9, as given in table 2. It is interesting to note that this multiplier had a narrow range from 0.318 to 0.822, increasing with increasing s_0. The entropy value varied from 0.318 Napier for site 6 to 0.822 Napier for site 9, implying that the latter site had the highest uncertainty associated with the side slope.

In order to determine if the CDF hypothesis was acceptable, the CDF was computed for all sites considering four different flow events, as shown for sample site S1 in figure 3, where s_0 = 1.75, x_0 = 4 cm, and W = 16 cm. It is

Table 2. Maximum slope and Lagrange multiplier.

s_0	λ_0
1.363	0.309
1.475	0.389
1.588	0.462
1.425	0.354
1.675	0.516
1.675	0.516
1.650	0.501
1.200	0.182
1.375	0.318

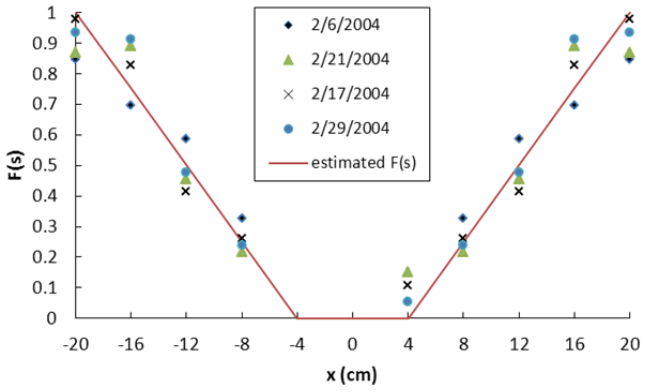

Figure 3. Cumulative probability distribution function of transverse slope for site S1.

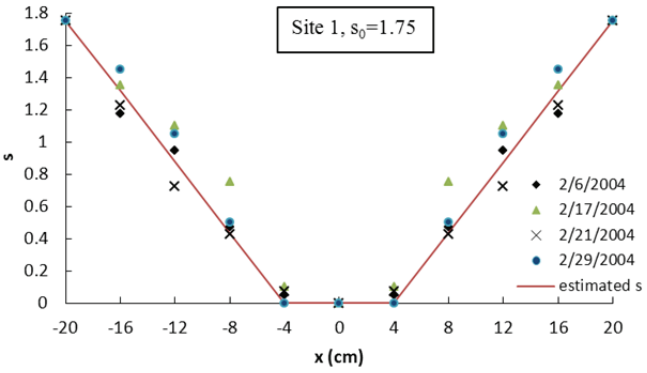

Figure 4. Distribution of transverse slope.

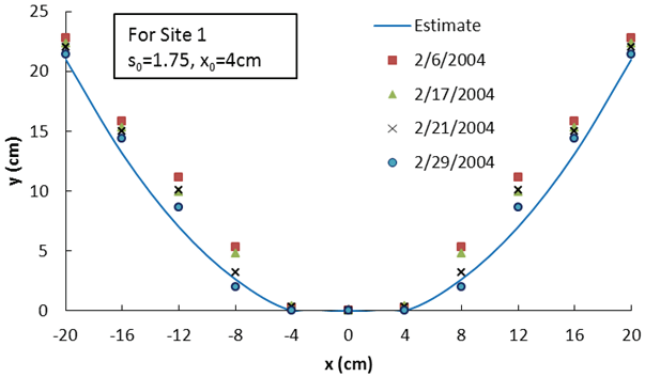

Figure 5. Furrow cross-section shape for site S1.

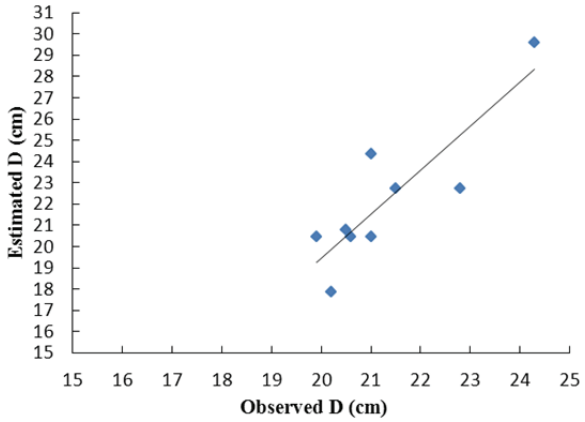

Figure 6. Comparison between observed and computed maximum flow depth.

seen that the computed CDF was not far from the observed CDF values. This same site will be used for illustrating the performance of the entropy-based derivations.The transverse slope was computed for all sites using equation 16, as shown in figure 4, for the cross-section at sample site S1 during the four flow events. It is seen that the transverse slope was satisfactorily predicted. The elevation to bank *y* was computed for all sites using equation 18a, as shown for the cross-section at site S1 in figure 5. The error in computed elevation [(estimated – observed)/observed] was below 30%, which is bit high, but in most cases it was below 20%. This means that the cross-section shape was satisfactorily predicted.

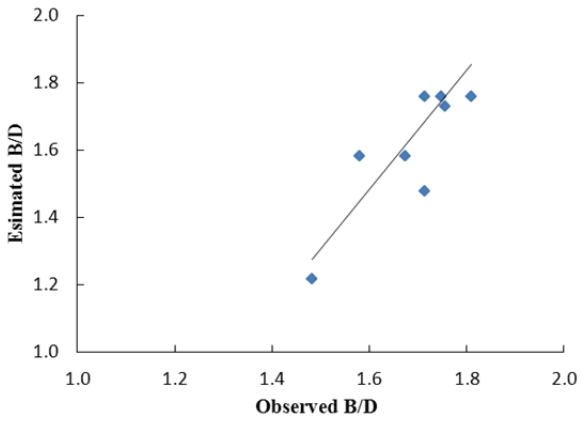

Figure 7. Comparison between computed and observed *B*/*D*.

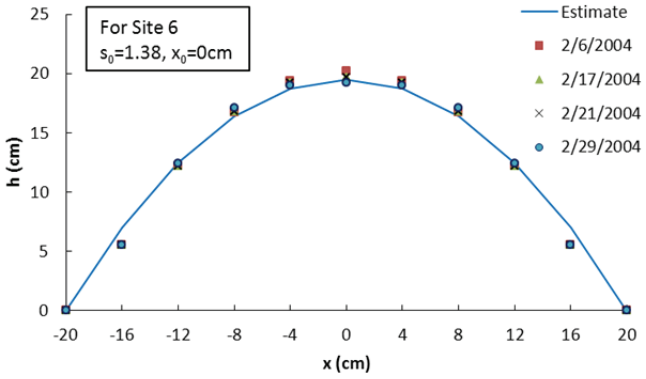

Figure 8. Transverse distribution of flow depth in the furrow cross-section.

For the initial furrow profile (6 February 2004 at 1:50 p.m.) with a flow rate of 0.2 L s^{-1} at site S1, $D = h_c = (s_0W/2) = (1.75 \times 26/2) = 22.75$ cm, which was slightly smaller than the observed value of 22.8 cm. More *D* values were computed using equation 19 for sites 1 to 9 for the initial furrow profile (6 February 2004 at 1:50 p.m.) with a flow rate of 0.2 L s^{-1}. The computed error varied from less than 0.2% to 22%, but it was below 10% for six of the nine sites. It was also seen that the estimated *D* was a little smaller than the observed *D* for small values, while the estimated *D* was larger than the observed *D* for large values, as shown in figure 6.

The width-depth ratio was computed using equation 21 for all sites, as shown in figure 7. It was observed that the estimation was bigger than the observation. The error in the computed width-depth ratio was below 18%, but it was well below 5% for five of the nine sites. The flow depth *h* was computed using equation 21a as a function of transverse distance, as shown for site S1 in figure 8. It was observed that the error in computed *h* was below 5%, but it exceeded 27% at one site. The flow cross-sectional area was computed using equation 23 for all sites. For the initial furrow profile (6 February 2004 at 1:50 p.m.) with a flow rate of 0.2 L s^{-1} at site S1, $A_0 = 2x_0D = 8 \times 22.8 = 172$ cm^2. The cross-sectional flow area was obtained with an error of less than 20%, but the error was less than 9% for seven of the nine sites, as shown in figure 9. The predicted cross-sectional area values were more susceptible to errors be-

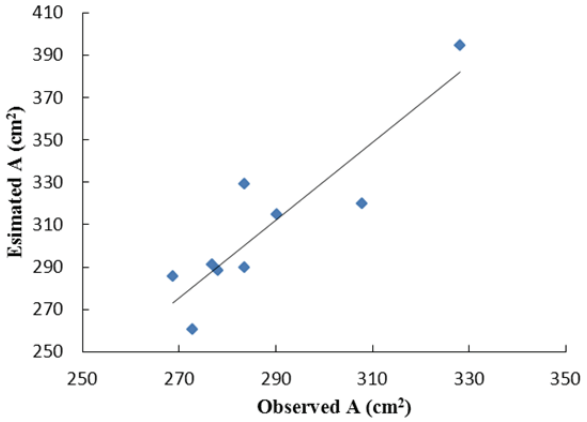

Figure 9. Comparison between computed and observed cross-section values.

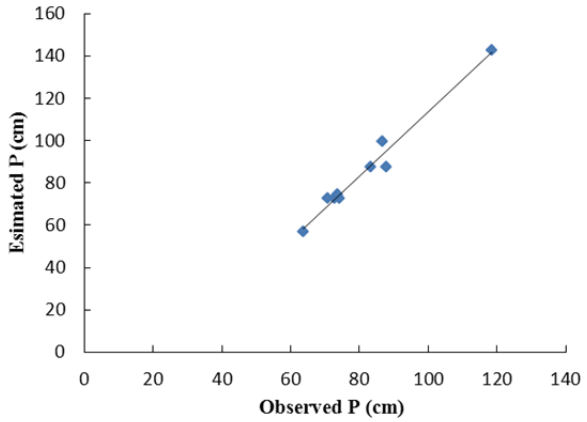

Figure 10. Comparison between computed and observed wetted perimeter values.

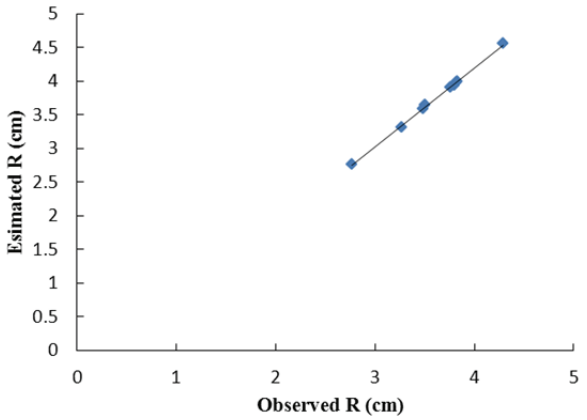

Figure 11. Comparison between computed and observed hydraulic radius values.

cause the flow depth was not as accurately predicted. The wetted perimeter was computed using equation 25 for all sites, as shown in figure 10. The error in the computed wetted perimeter was less than 20%, but it was below 5% for six of the nine sites. The hydraulic radius was computed using equation 26 for all sites, as shown in figure 11, which shows that the computed values of the hydraulic radius were close to the observed values. The better agreement may be because the wetted perimeter was satisfactorily predicted.

Conclusions

The following conclusions are drawn from this study: (1) Using no information on furrow geometry and using a simple hypothesis on the cumulative probability distribution of side slope, entropy theory leads to simple expressions for the various geometric parameters. (2) Comparison of computed values of these parameters with observed values in field laboratory experiments at nine sites shows that the computed values are in satisfactory agreement with the observed values. (3) Satisfactory agreement between the computed and observed values suggests that entropy theory has potential in the modeling and design of irrigation systems.

Acknowledgments

The author gratefully acknowledges the data provided by Dr. D. R. Mailapalli, who conducted field laboratory experiments on furrows at the Indian Institute of Technology in Kharagpur, India. Dr. Mailapalli was quite generous to share details of the experimental setup and the experiments. Ms. Huijuan Cui helped with the numerical calculations and graphs, and her help is sincerely appreciated.

References

Abrahams, A. D., A. J. Parson, and S.-H. Luk. 1986. Resistance to overland flow on desert hill slopes. *J. Hydrol.* 88(3-4): 343-363.

Chow, V. T. 1959. *Open Channel Hydraulics.* New York, N.Y.: McGraw-Hill.

Elliott, R. L., W. R. Walker, and G. V. Skogerboe. 1983. Furrow irrigation advance rates: A dimensional approach. *Trans. ASAE* 26(6): 1722-1725, 1731.

Fangmeier, D. D., and M. K. Ramsey. 1978. Intake characteristics of irrigation furrows. *Trans. ASAE* 21(4): 696-700, 705.

Foster, G. R., and L. J. Lane. 1983. Erosion by concentrated flow in farm fields. In *Proc. D.B. Simons Symposium on Erosion and Sedimentation*, 9.56-9.82. Fort Collins, Colo.: Colorado State University.

Henderson, F. M. 1966. *Open Channel Flow*. New York, N.Y.: Macmillan.

Jaynes, E. T. 1957. Information theory and statistical mechanics. *Physical Review* 106(4): 620-630.

King, H. W. 1939. *Handbook of Hydraulics*. New York, N.Y.: McGraw-Hill.

Lane, L. J., and M. A. Nearing, eds. 1989. USDA Water Erosion Prediction Project: Hillslope profile model documentation. NSERL Report No. 2. West Lafayette, Ind.: USDA-ARS National Soil Erosion Research Laboratory.

Mailapalli, D. R. 2006. Development and testing of physically based model for simulating flow and sediment transport in furrow irrigation. Unpublished PhD diss. Kharagpur, India: Indian Institute of Technology.

Shannon, C. E. 1948. A mathematical theory of communication. *Bell System Tech. J.* 27(3): 379-423.

Singh, V. P. 2011. Hydrologic synthesis using entropy theory: A review. *J. Hydrol. Eng.* 16(5): 421-433.

SCS. 1983. Section 15, Chapter 5: Furrow irrigation. In *National Engineering Handbook*. Washington, D.C.: USDA Soil Conservation Service.

Trout, T. J. 1991. Furrow geometric parameters. *J. Irrig. and Drain. Eng.* 117(5): 613-634.